CHAPTER 275

COASTAL MORPHODYNAMIC INSTABILITIES

Albert Falqués, Amadeu Montoto and Vicente Iranzo [1]

Abstract

An initially plane beach is considered with waves incoming obliquely. For this basic steady state the Longuet-Higgins solution is used to give set-up and longshore current. The beach is assumed to be erodible. Then, a stability analysis is performed considering infinitesimal disturbances in the current, the free surface and the sea bottom. The basic undisturbed state is found to be unstable giving rise to topographic features similar to oblique or transverse bars and to a meandering in the longshore current. Some comparison with the erlier work by Christensen et al., 1994, is made.

1. Introduction

Beach topography often show tridimensional patterns with some kind of recurrence or rhythmicity in the alongshore direction. Typical examples are oblique/transverse bar systems, crescentic longshore bars, ridge and runnel systems, etc. The explanation for rhythmic topography has followed to main theoretical approaches: i) the infragravity wave influence on sediment transport and distribution (see for instance, Holman and Bowen, 1982) and ii) the morphodynamic instability of the surf-zone under the action of the incoming waves and the longshore current (see Hino, 1974 and Christensen et al., 1994). The basic idea in this latter approach is as follows. Given an initial beach topography, the incoming waves produce some currents. This currents carry sediments and this sediment transport can produce changes in the topography which in turn affects the incoming wave field and the current. In this way there is a feedback and if some perturbation within this loop produces a positive feedback the perturbation will start to grow. Then an instability arises leading to topographic features. In earlier works (Falqués et al., 1996a, Falqués et al., 1996b) the instability of the current-sea bed system

[1] Departament de Física Aplicada, Universitat Politècnica de Catalunya, 08034 Barcelona, Spain

keeping fixed the incoming wave field was analyzed (bed-flow instability). The aim of the present contribution is to include the effect of the perturbations in the incoming wave field. In this way we reproduce and extend the results of Hino, 1974, and Christensen et al., 1994, with a different numerical model. Special attention is paid to the bar shape and orientation, the systematic trends with respect to bottom friction and other parameters and the influence of lateral momentum diffusion.

2. Model equations

Since our aim is to look at large 2D horizontal patterns in the near shore, a 2D shallow water model with time-average over incoming wave period is considered. As governing equations we take the momentum equations:

$$\frac{\partial \vec{v}}{\partial t} + \vec{v} \cdot \nabla \vec{v} + g \nabla z_s - \frac{\vec{\tau}_b}{\rho \zeta} - \vec{\mathcal{V}} = \frac{1}{\rho \zeta} \nabla \cdot S \tag{1}$$

the mass conservation equation

$$\frac{\partial \zeta}{\partial t} + \nabla \cdot (\zeta \vec{v}) = 0 \tag{2}$$

and the sediment conservation equation

$$\frac{\partial z_b}{\partial t} + \nabla \cdot \vec{q} = 0 \tag{3}$$

A cartesian coordinate system is assumed with x cross-shore, y alongshore and z vertical upwards (see Fig.1). $\zeta = z_s - z_b$ is the total depth, $\vec{\tau}_b$ the bottom friction and S is the radiation stress tensor. The lateral momentum diffusion terms read:

$$\mathcal{V}_i = \frac{1}{\zeta} \sum_{j=1}^{2} \frac{\partial}{\partial x_j} [\nu_t \zeta (\frac{\partial v_i}{\partial x_j} + \frac{\partial v_j}{\partial x_i})] \qquad i = 1, 2 \tag{4}$$

Here, $x_1 = x$ and $x_2 = y$. The sand transport is parametrized by the formula:

$$\vec{q} = \nu |\vec{v}|^m (\frac{\vec{v}}{|\vec{v}|} - \gamma \nabla h) \tag{5}$$

where h is any bottom perturbation with respect to equilibrium and where the term $\gamma \nabla h$ takes account of the tendency of the sand to move downslope. The exponent m has been set to 3 which is suitable for bed-load transport and $\gamma \sim 1$. Now we are going to perform a linear stability analysis for the system of equations 1, 2, 3. First, let us consider a basic steady equilibrium. In this state we assume waves incoming obliquely on the beach (see Fig. 2). The equilibrium consists of a set-up/down in the mean water level and a longshore current. For simplicity so that to be able to use analytical expressions, we will use the Longuet-Higgins solution (Horikawa, 1988). Thus, we assume a saturated surf zone, $H = \gamma_b \zeta$, $x \leq X_b$. The bottom friction (weak current and small angle) is given by

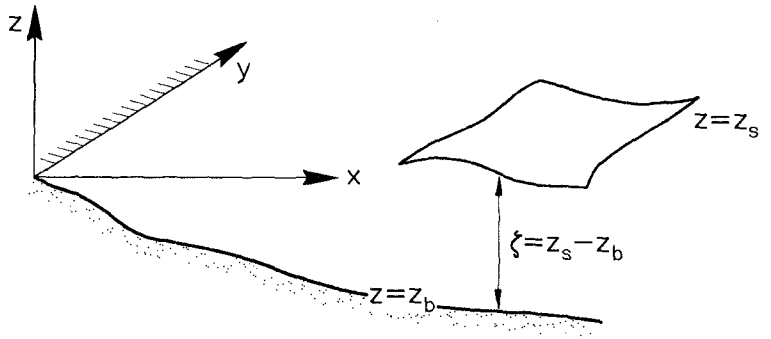

Figure 1: coordinate system.

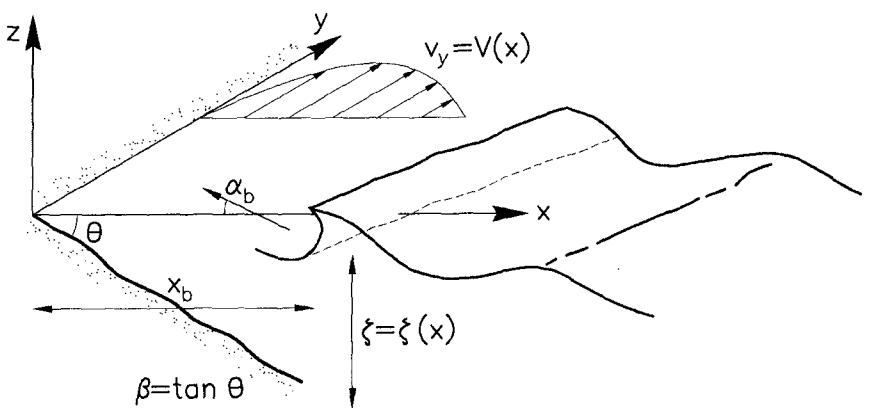

Figure 2: basic steady equilibrium.

$$\tau_{bx} = -\frac{4}{\pi}\rho c_f u_0 v_x \qquad , \qquad \tau_{by} = -\frac{2}{\pi}\rho c_f u_0 v_y \tag{6}$$

and the eddy viscosity reads $\nu_t = Nx\sqrt{g\zeta}$.

Consider now a small perturbation on the basic equilibrium of the form:

$$\vec{v} = (0, V(x)) + (\hat{u}(x), \hat{v}(x))e^{\sigma t + iky}$$

$$z_s = z_s^0(x) + \hat{\eta}(x)e^{\sigma t + iky}$$

$$z_b = z_b^0(x) + \hat{h}(x)e^{\sigma t + iky}$$

where $\lambda = 2\pi/k$ is the wavelength or the alongshore spacing of the growing bedforms. Then, by linearizing equations 1, 2, 3 we obtain:

$$\frac{\partial u}{\partial t} + V\frac{\partial u}{\partial y} + g\frac{\partial \eta}{\partial x} = [\frac{\tau_{bx}}{\rho\zeta}]^{\mathcal{L}} + [\mathcal{V}_x]^{\mathcal{L}} + [\frac{1}{\rho\zeta}(\frac{\partial S_{xx}}{\partial x} + \frac{\partial S_{xy}}{\partial y}]^{\mathcal{L}} \tag{7}$$

$$\frac{\partial v}{\partial t} + V\frac{\partial v}{\partial y} + \frac{dV}{dx}u + g\frac{\partial eta}{\partial y} = [\frac{\tau_{by}}{\rho\zeta}]^{\mathcal{L}} + [\mathcal{V}_y]^{\mathcal{L}} + [\frac{1}{\rho\zeta}(\frac{\partial S_{yx}}{\partial x} + \frac{\partial S_{yy}}{\partial y}]^{\mathcal{L}} \tag{8}$$

$$\frac{\partial \eta}{\partial t} - \frac{\partial h}{\partial t} + [\nabla \cdot (\zeta\vec{v})]^{\mathcal{L}} = 0 \tag{9}$$

$$\frac{\partial h}{\partial t} + [\nabla \cdot \vec{q}]^{\mathcal{L}} = 0 \tag{10}$$

These equations are too long to be written here in detail in such a way that we abbreviate 'linear part of' by

$$[.]^{\mathcal{L}}$$

The perturbation in the radiation stress terms will be called bed-surf terms since they describe the perturbation in the incoming wave field due to growing bedforms. The perturbation in the wave refraction should be also included in the bed-surf terms but this has not been done in the present work. The remaining terms in the linearized equations if bed-surf effect is neglected will be called bed-flow terms since they describe the perturbation in the current due to the growing bedforms if the forcing by the waves is kept fixed.

Before solving the linear problem, a scaling and some non-dimensional parameters will be introduced. As horizontal lengthscale, the width of the surf zone, $L_H = X_b$, is choosen and $L_V = \beta X_b$ will be the vertical scale where β is the beach slope (see Fig.3). The velocity scale is the scale for the Longuet-Higgins model,

$$U = \frac{5\pi}{16}\frac{\gamma_b}{c_f}\sqrt{g\zeta_b}\beta' \, sin\, \alpha_b$$

where β' is the effective beach slope including set-up and α_b is the wave angle with rescect to the cross-shore at breaking. Two time scales appear , $T_h = L_H/U$, $T_m = L_H L_V/Q$, where $Q = \nu U^m$ is the scale for sediment transport. The second one arises in a natural way from the sediment conservation equation (10) and will be called morphological time scale. It is the scale at which bedforms are expected to grow. The first one will be called hydrodynamical time scale and it is much shorter than the other one.

The variables are made nondimensional by means of:

$$(x, y) = L_H(x', y') \quad , \quad z_b = L_V z_b' \quad , \quad z_s = \frac{U^2}{g} z_s'$$

$$(u, v) = U(u', v') \quad , \quad t = T_m t'$$

Then, we deal with non-dimensional linear equations with the following dimensionless parameters. First a nondimensional wavenumber and growth rate, $k' = kL_H, \sigma' = \sigma T_m$. Also, the breaking index, γ_b, the wave angle at breaking, α_b and the viscosity parameter, N, appear. The parameter related to the tendency of the sedimend to go downslope now become $\gamma' = \gamma\beta$. An important parameter is the characteristic Froude number of the longshore current, $F = U/\sqrt{gL_V}$ and the frictional parameter, $r = c_f/\beta$. Finally, the ratio between both time scales, $\epsilon = T_h/T_m$, is very small but not set to 0 (which is usually called quasi-steady hypothesis. See 'response time concept' in Christensen et al, 1994). In this way, the model allows for the computation of purely hydrodynamic instabilities like shear waves or even for the possible interaction between both kind of instabilities. However, we have focussed only in morphological instabilities for the present contribution. Hereinafter, nondimensional quantities will be handled dropping accents for simplicity.

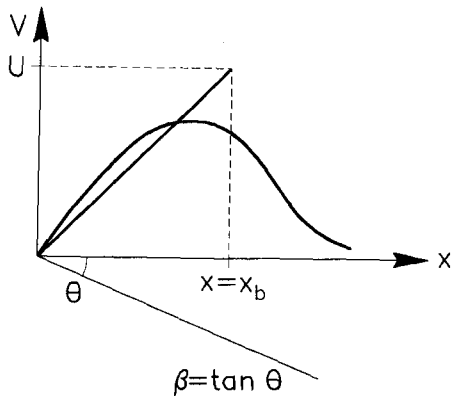

Figure 3: scaling.

Finally, equations (7),(8),(9) and (10) result in an eigenproblem where the eigenvalue is the growthrate, σ, and the eigenfunctions the perturbations $(\hat{u}(x), \hat{v}(x), \hat{\eta}(x), \hat{h}(x))$. This problem is discretized by a numerical spectral method. In the next section, an indication is given of the solution procedure.

3. Numerical method

For simplicity, we will ilustrate the numerical method by means of a simpler eigenproblem than (7)-(10). Consider the differential equation

$$p(x)u''(x) + q(x)u'(x) + r(x)u(x) = \sigma u(x) \qquad 0 < x < \infty \tag{11}$$

with boundary conditions $u(0) = u(\infty) = 0$. Here, σ is the eigenvalue and $u(x)$ the eigenfunction.

The method uses an expansion in Chebyshev polynomials and a

transformation from $[0, \infty)$ to $[-1, 1)$. First, this map is given by

$$x = \phi(z) = l\frac{1-z}{1+z} \tag{12}$$

(see Falqués and Iranzo, 1994).

Second, an expansion in Chebyshecv polynomials is assumed:

$$u(x) = \sum_{n=0}^{N} \hat{u}_n T_n(z) = \sum_{n=0}^{N} \hat{u}_n T_n(\phi^{-1}(x)) \tag{13}$$

The following step is to find a combination of Chebyshev polynomials which verify the boundary conditions. The N-1 functions which satisfy this requirement are:

$$g_n(x) = T_n(\phi^{-1}(x)) - \frac{1}{2}(1+(-1)^n)T_0(\phi^{-1}(x)) - \frac{1}{2}(1+(-1)^{n+1})T_1(\phi^{-1}(x)) \tag{14}$$

where $n = 2, 3, ..., N$. Then, expansion (13) is substituted by

$$u(x) = \sum_{n=2}^{N} \hat{u}_n g_n(x) \tag{14}$$

where the unknowns (eigenvector) are the $N-1$ coefficients $\hat{u}_2, ...\hat{u}_N$.

Now, to discretize equation (11) we will apply collocation at the Gauss-Lobatto nodes $z_i = cos(\pi i/N)$ transformed by the map (12) (Falqués and Iranzo, 1994). For this purpose, the first step is to know the values of g_n at the nodes. This is given by the martix $G_{ij} = g_j(x_i)$, so that

$$u(x_i) = \sum_{n=2}^{N} G_{in}\hat{u}_n$$

In a similar way, the first derivative of u will be given by a matrix G' :

$$u'(x_i) = \sum_{n=2}^{N} G'_{in}\hat{u}_n$$

where $G'_{in} = g'_n(x_i)$ can be computed by using the derivatives of the Chebyshev polynomials and the map (12). Similarly, the second derivative will be computed by

$$u''(x_i) = \sum_{n=2}^{N} G''_{in}\hat{u}_n$$

where $G''_{in} = g''_n(x_i)$ can also be computed by means of the derivatives of the Chebyshev polynomials and the map (12). Explicit expressions of the

derivatives of Chebyshev polynomials combined with (12) can be found in Falqués and Iranzo, 1994.

Finally, after performing collocation at x_i, $i = 1...N-1$ the discretized eigenproblem reads:

$$p(x_i)\sum_{k=2}^{N} G''_{ik}\hat{u}_k + q(x_i)\sum_{k=2}^{N} G'_{ik}\hat{u}_k + r(x_i)\sum_{k=2}^{N} G_{ik}\hat{u}_k = \sigma\sum_{k=2}^{N} G_{ik}\hat{u}_k$$

where the eigenvector is $(\hat{u}_2...\hat{u}_N)$.

4. Results

One of the drawbacks of Hino model, 1974, without the quasisteady hypothesis, i.e., hydrodynamic instabilities out of control, has been solved. All hydrodynamic instabilities could be identified as shear waves with a clear maximum in the $\sigma - k$ curve. Shear waves have growthrates an order ϵ^{-1} larger than bed wave growthrates. By comparison with other models (Falqués and Iranzo, 1994) they could be recognized. Usually, however, when a realistic friction and viscosity parameters are choosen, no hydrodynamic instabilities appear. Figure 4 shows the nondimensional growth rate $Re(\sigma)$ as a function of the wavenumber k, for three different cases. In one set of curves only bed-flow terms were kept in the equations while in the other set the full equations (bed-flow + bed-surf) were considered. It can be seen that bed-surf, that is, the effect of the wave field perturbation enhances significantly the instability. This was also found by Christensen at al., 1994. Also, bed-surf gives shorter spacing between the bedforms. The imaginary part of σ is not shown here. It is negative and of order one. This means that the topographic waves migrate downcurrent with a speed of the order L_H/T_m.

Regarding the shape of the topographic features, two kind of bedforms were found. First what we call current dominated bedforms. In this case, the shape of the bars looks very similar when only bed-flow terms were taken or when bed-flow and bed-surf were considered. The bars are upcurrent rotated, very oblique (a small angle with the shoreline of the order of 10°). These topographic waves come out in the case of a relatively high characteristic Froude number, say $F > 0.6$ (note that this is not the maximum local Froude number which can be smaller). According to

$$F = \frac{U}{\sqrt{g\zeta_b}} = \frac{5\pi}{16}\frac{\gamma_b}{\sqrt{1+0.375\gamma_b^2}}\frac{sin\,\alpha_b}{r} \tag{15}$$

this corresponds to small frictional parameter, r, and large angle, α_b. Figure 5 shows how the bottom perturbations with only bed-flow and with bed-flow and bed-surf look quite similar. Figure 7 shows the full equation bedform when the basic slope is added to the perturbation.

Second, we found what we call wave-dominated bedforms. In this case the shape of the bars with only bed-flow or with bed-flow and bed-surf looks

quite different. With only bed-flow they are similar to alternate bars in a river and in the other case they are similar to transverse bars slighly upcurrent rotated (see Fig.6). Figure 8 shows, in this case, the total topography with bed-flow and bed-surf. Wave-dominated bedforms appear for small Froude number, say $F < 0.6$, that is, for large frictional parameter and small angle.

An important issue of morphological models for rhythmic features is the alongshore spacing or wavelength. This is found by looking at the fastest growing wavenumber, i.e., the maxima in the σ_r, k curves for different values of the parameters. From experimental data (usually from the spacing between rip currents assumed to be related to rhythmic topography) the wavelength to surf zone width ratio is in the order $\lambda/X_b \sim 1.5 - 8$. The mean value is between 3 and 4 (Sasaki and Horikawa, 1975). Christensen et al., 1994 found a ratio about 6. In our modelling this ratio ranges between 1 and 7, depending on the frictional parameter, r, and on the wave angle, α_b. It decreases with increasing r and with decreasing α_b (see Fig. 9).

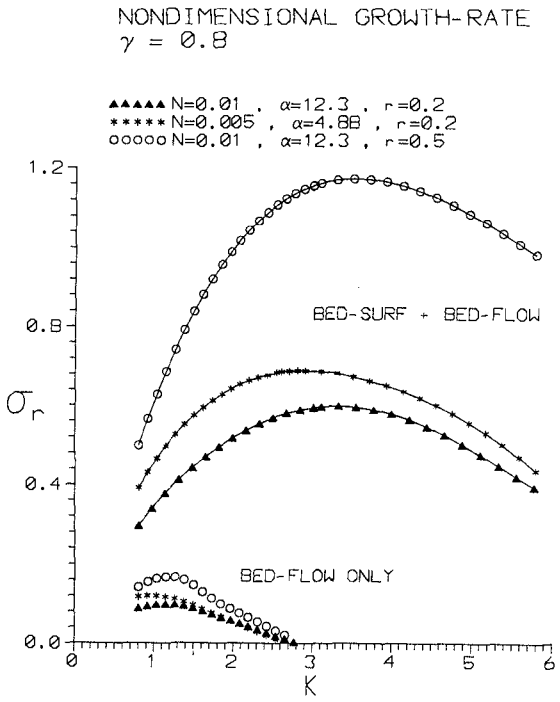

Figure 4: growthrate as a function of wavenumber for three sets of parameters. $F = 0.3, \epsilon = 0.001, \gamma = 0.01$.

The growing bedforms produce a meandering in the longshore current. According to our simulation, the current is deflected offshore over the shoals

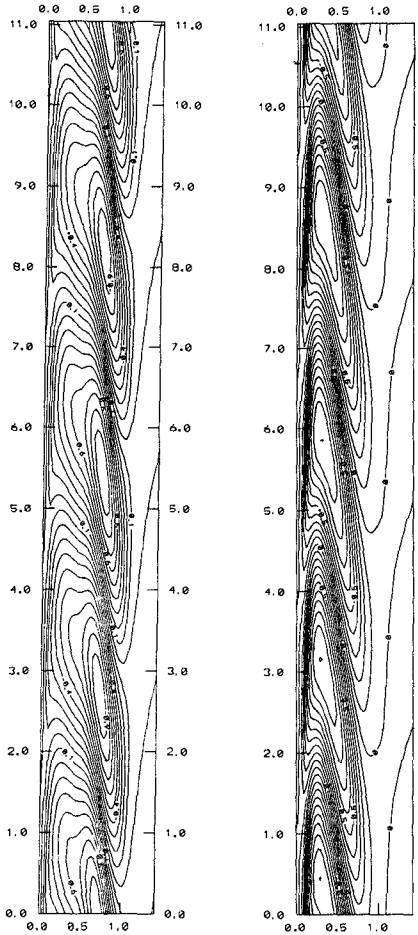

Figure 5: perturbation in the bottom for $r = 0.1, \alpha_b = 12.3^o, F = 0.8, N = 0.005, \gamma_b = 0.4, k = 1.14$. Right: only bed-flow, left= bed-flow and bed-surf. In this plot the current runs from the bottom to the top.

and inshore over the pools (see Fig.10). Thinking of rip currents, this is in contrast with many observed rip currents. But two things have to be taken into account. First this is the initial growth. It could be that for finite amplitude features this behaviour would be reversed leading to a non-linear saturation of the growth. Second, these are not exactly rip currents but just the

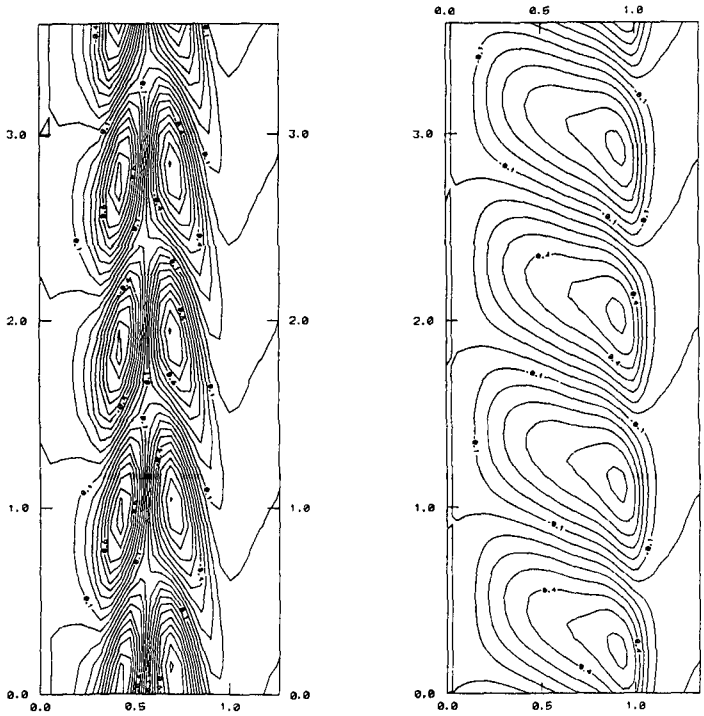

Figure 6: perturbation in the bottom for $r = 0.5, \alpha_b = 12.3^o, F = 0.16, N = 0.005, \gamma_b = 0.4, k = 3.5$. Right: only bed-flow, left= bed-flow and bed-surf. In this plot the current runs from the bottom to the top.

deflection of the longshore current. Also Christensen et al., 1994, found the same behaviour.

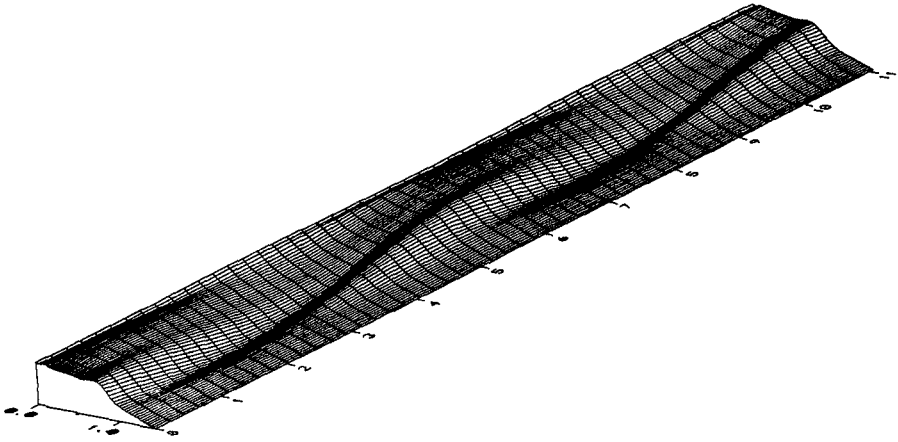

Figure 7: bottom topography for $r = 0.1, \alpha_b = 12.3^o, F = 0.8, N = 0.005, \gamma_b = 0.4, k = 1.14$. Basic slope plus perturbation (with arbitrary amplitude since we are dealing with a linear problem). Current running from left to right.

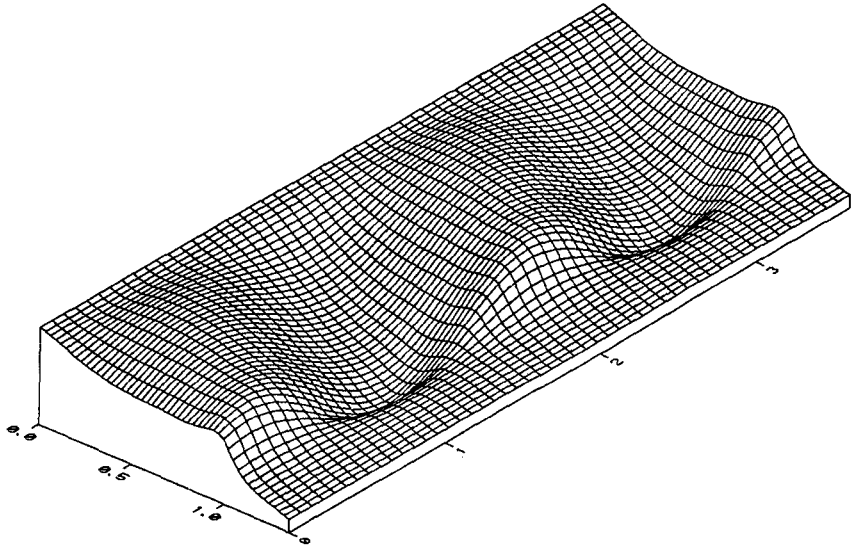

Figure 8: bottom topography for $r = 0.5, \alpha_b = 12.3^o, F = 0.16, N = 0.005, \gamma_b = 0.4, k = 3.5$. Basic slope plus perturbation. Current running from left to right.

5. Conclusions

It has been shown that the topography of a plane beach can be unstable due to the interaction with the incoming waves and the longshore current. The effect of the perturbation on the waves (bed-surf) turns out to be the most de-stabilizing. This is in line with Christensen et al., 1994. The instability produces the growth of upcurrent rotated bars which is also in agreement with the earlier work of Christensen et al. However, as these authors pointed out, this is sometimes in agreement with the observed bars in the field and sometimes is in contrast. We found two kind of topographic features: i) 'current dominated' (large angle, small friction) and ii) 'wave dominated' (small angle, large friction). Instead of fixed values of the alongshore spacing

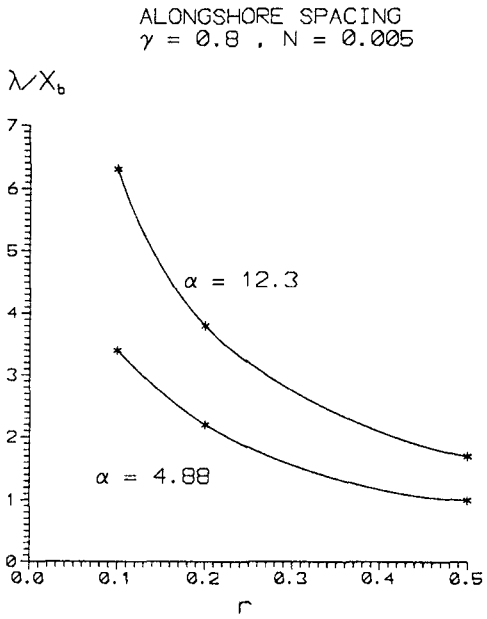

Figure 9: Alongshore spacing of the topographic waves.

λ/X_b (4 in the case of Hino and 6 in the case of Christensen et al.,) our alongshore spacing ratio ranges from 1 to 7, decreasing for increasing r, and depending on α_b and N. Finally, the growing bedforms produce a small meandering of the longshore current with an offshore deflection over the shoals. This can be a little surprising but it is also in line with earlier results of Christensen et al. Clearly, more research is needed to clarify the mechanism which produces this perturbed flow in combination with the perturbation in the set-up.

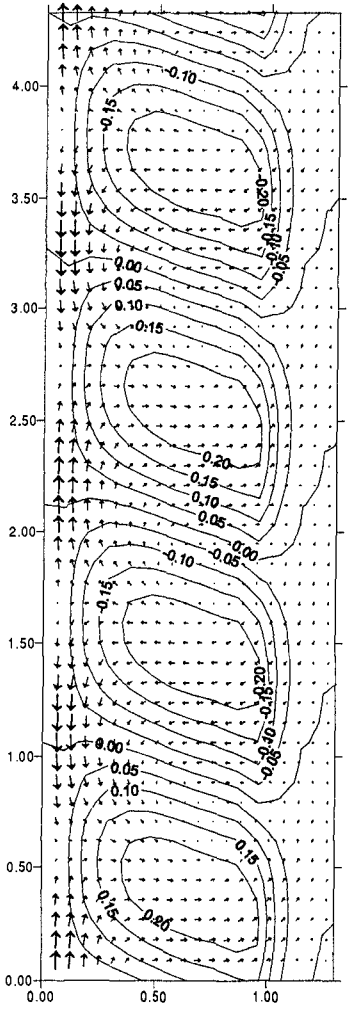

Figure 10: wave-dominated bedform and the perturbation produced on the current. Note the offshore deflection over the shoals. $r = 0.2, \alpha_b = 4.88^o, F = 0.3, N = 0.005, \gamma_b = 0.8$. Basic current running from bottom to top.

Acknowlodgements

This work has been funded by the Spanish government (DGICYT) under contract PB93-0948. Part of the work of A.Falqués has been done in Utrecht University (IMAU) funded by RIKZ (Netherlands Institute of Coastal Management).

References

Christensen,E.,Deigaard,R.and Fredsoe,J.,1994. Sea bed stability on a long straight coast 24th Int. Conf. Coastal Engineering, 1865-1879.

Falqués,A. and Iranzo,V.,1994. Numerical simulation of vorticity waves in the nearshore. J.Geophys. Res., 99, 825-841.

A.Falqués, A.Montoto and V.Iranzo, 1996a. Bed-Flow instability of the longshore current. Cont.Shelf Res. (in press).

A.Falqués, A.Montoto, V.Iranzo, 1996b. Bed-flow instability of longshore currents. XXI European Geophysical Society General Assembly, The Hague, 6-10 May 1996.

Hino,M.,1974. Theory on formation of rip-current and cuspidal coast 14th Int. Conf. Coastal Engineering, 901-919.

Holman,R.and Bowen,A.,1982. Bars, bumps, and holes: models for the generation of complex beach topography J.Geophys. Res.,87,457-468.

K.Horikawa(editor), 1988. Nearshore Dynamics and Coastal Processes. University of Tokio Press.

Sasaki,T. and Horikawa,K., 1975. Nearshore current system on a gently sloping bottom. Coastal Eng. in Japan, 18, 123-143.